Cell PRESS
Chemistry & Biology
Brief Communication

Two Molecules of Lobophorolide Cooperate to Stabilize an Actin Dimer Using Both Their "Ring" and "Tail" Region

J. Craig Blain,[1,3] Yee-Foong Mok,[1] Julia Kubanek,[2] and John S. Allingham[1,*]
[1]Department of Biochemistry, Queen's University, Kingston, ON K7L 3N6, Canada
[2]School of Biology & School of Chemistry and Biochemistry, Georgia Institute of Technology, Atlanta, GA 30332, USA
[3]Present address: Department of Genetics, Harvard Medical School, Boston, MA 02115, USA
*Correspondence: allinghj@queensu.ca
DOI 10.1016/j.chembiol.2010.06.010

SUMMARY

Actin filament-disrupting marine macrolides are promising templates from which to design therapeutics against cancer and other diseases that co-opt the actin cytoskeleton. Typically, these macrolides form either a 1:1 or 2:1 actin-macrolide complex where their aliphatic side chain, or "tail," has been reported to convey the major determinant of cytotoxicity. We now report the structure of the marine macrolide lobophorolide bound to actin with a unique 2:2 stoichiometry in which two lobophorolide molecules cooperate to form a dimerization interface that is composed entirely of the macrolide "ring" region, and each molecule of lobophorolide interacts with both actin subunits via their ring and tail regions to tether the subunits together. This binding mode imposes multiple barriers against microfilament stability and holds important implications for development of actin-targeting drugs and the evolution of macrolide biosynthetic enzymes.

INTRODUCTION

Proper regulation of actin polymerization is central to many processes in eukaryotic cells (Pollard and Borisy, 2003) and a large number of diverse natural products have been found that bind to actin and disrupt its polymerization dynamics, leading to high cytotoxicity in numerous cell types (Allingham et al., 2006). Many actin-binding compounds are monomeric macrolides that consist of a highly variable 24- to 26-membered macrolactone ring with a long aliphatic side chain (tail) terminating with an *N*-methyl-vinylformamide moiety (see Figure S1 available online). These compounds bind the barbed end of actin to form a 1:1 actin-macrolide complex that disrupts longitudinal interactions between adjacent actin filament subunits, allowing sequestration of globular actin (G-actin), severing of filamentous actin (F-actin), and capping of filament ends (Allingham et al., 2005; Klenchin et al., 2003). X-ray crystal structures of these macrolides bound to actin have revealed common actin-binding interfaces for defined regions of different macrolides and have provided some molecular explanations for their effects (Allingham et al., 2005; Hirata et al., 2006; Klenchin et al., 2003). Most of the observed actin-binding interface commonality among different macrolides involves the tail region, suggesting that the tail is a major contributor to their high affinity toward actin and cytotoxic functionality (Allingham et al., 2005; Hirata et al., 2006). With this information, synthetic mimetics comprising mainly the tail component of these macrolides have recently been developed with the potential to act as therapeutics for diseases that co-opt the actin cytoskeleton, such as cancer metastasis and certain microbial infections (Perrins et al., 2008). A deeper understanding of the contributions of the ring component to their inhibition of actin polymerization could guide refinement and elaboration of these mimetics and will rely on structure-function analysis of structurally unprecedented compounds that display potent cytotoxicity.

The marine sponge *Theonella swinhoei* produces a barbed end binding macrolide, named swinholide, that consists of a 44-membered dimeric cyclic lactone possessing two identical pyrone ring-terminated side chains, giving the molecule a 2-fold axis of symmetry (Figure 1A) (Kobayashi et al., 1990). As a result, swinholide forms an actin-macrolide complex with 2:1 stoichiometry in which each side chain accesses the barbed end cleft of a different actin molecule (Bubb et al., 1995; Klenchin et al., 2005). Interestingly, the brown alga *Lobophora variegata* produces a macrolide called lobophorolide that is essentially half of the dimeric swinholide (Figure 1A) (Kubanek et al., 2003). It consists of a 22-membered macrolactone ring attached to a pyrone ring-terminated aliphatic side chain, and thus is structurally unprecedented relative to the other monomeric macrolides described above. Both lobophorolide and swinholide display sub-μM antifungal activity and are highly cytotoxic to a variety of cancer cell lines, where swinholide's cytotoxic activities are dependent on the integrity of its ring structure (Kobayashi et al., 1994; Kubanek et al., 2003). Given its similarity to a portion of swinholide, lobophorolide has been postulated to be a barbed end targeting macrolide (Allingham et al., 2006); however, this has not been confirmed. To elucidate the basis for lobophorolide's cytotoxicity, we determined its structure bound to G-actin at 2.0 Å resolution by X-ray crystallography and analyzed its effects on purified actin polymers in vitro.

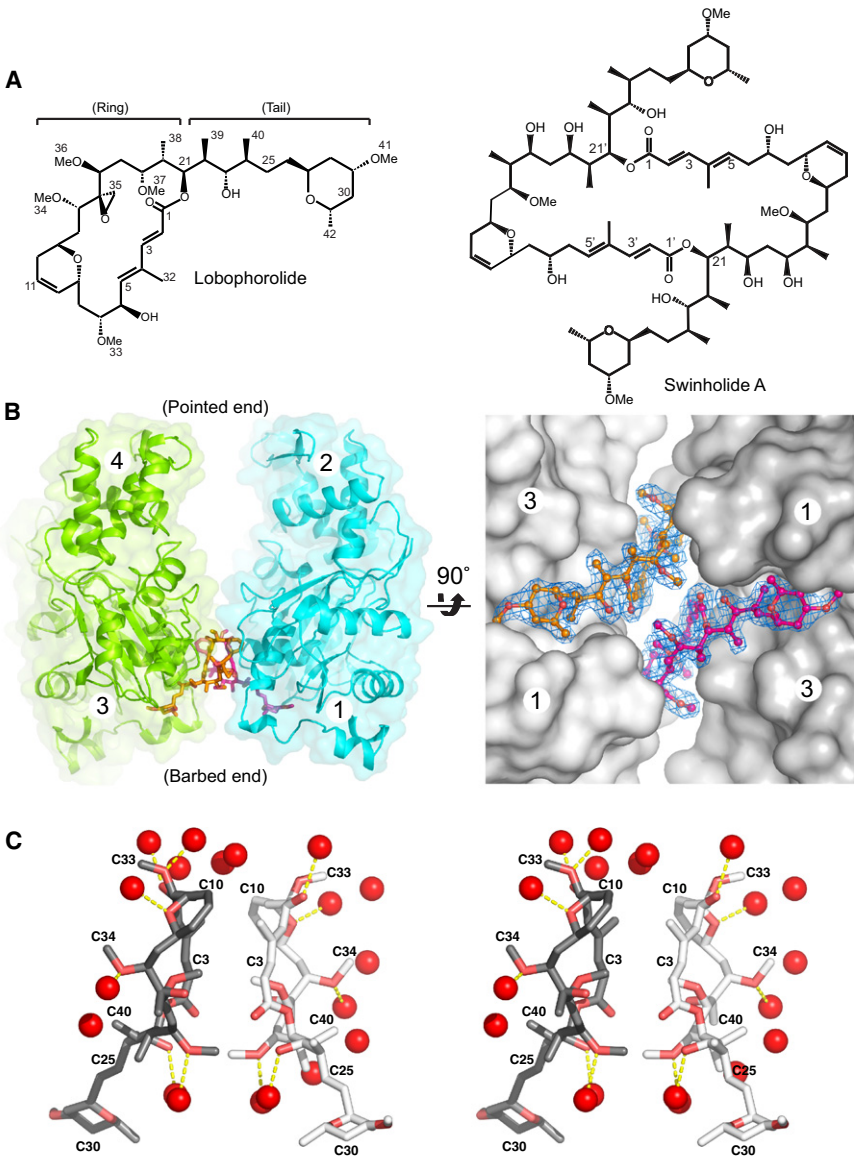

Figure 1. Chemical and Actin-Bound Structures of Lobophorolide

(A) The "ring" and "tail" components of lobophorolide are indicated. The chemical structure of swinholide A is shown for comparison.

(B) Two actin subunits (green and cyan) are stabilized as a complex with 2-fold rotational symmetry by two lobophorolide molecules (magenta and orange sticks). Subdomains 1 to 4 are labeled. The F_o-F_c electron density omit map contoured at 3 σ for each lobophorolide molecule is shown.

(C) Stereo view of the two lobophorolide molecules and nearby waters (red spheres) shows the exclusion of water molecules at the interface formed by their macrolactone rings. Dotted lines indicate bonds with waters.

RESULTS AND DISCUSSION

Overview of the Actin-Lobophorolide Complex

The asymmetric unit of the actin-lobophorolide crystal contains a complex in which two lobophorolide molecules mediate formation of a nonphysiological actin dimer with noncrystallographic 2-fold rotational symmetry (Figure 1B; Table S1). Electron density maps for both lobophorolide molecules are unambiguous and are in agreement with the stereochemical assignments made by Kubanek and colleagues (Kubanek et al., 2003), and sedimentation velocity analysis confirmed the formation of an actin dimer ($s_{20,w}$ = 5.1) in solution upon addition of lobophorolide to monomeric G-actin (Figure S2). This complex appears to be stabilized by lobophorolide in two ways: 1) the macrolactone ring of each lobophorolide molecule is oriented so that each actin-lobophorolide unit presents a self-complementary hydrophobic surface, creating a 300 Å^2 dimerization interface that is stabilized by the hydrophobic effect and van der Waals contacts (Figure 1C), and 2) each lobophorolide molecule interacts with both actin subunits to help tether the complex together and bury a combined 2603 Å^2 of molecular surface area on the actin subunits.

No other monomeric macrolides are known to form such a quaternary complex; however, the actin-lobophorolide complex is strikingly similar to the 2:1 actin-swinholide A and actin-rhizopodin complexes, with the exception that the orientation of their actin subunits differ by a twist angle of approximately 18° and −22°, respectively (Figure S3; Hagelueken et al., 2009; Klenchin et al., 2005). A global alignment of both actin subunits for the lobophorolide and swinholide complexes provides a view of the extensive similarities in the three-dimensional space occupied by analogous atoms of each macrolide (Figure 2A). It also reveals that the interface between the two lobophorolide molecules occupies the same position as the site where the macrocycle of swinholide crisscrosses to produce the figure-eight-like conformation that allows both of its side chains to interact with the two actin molecules. Analogously to swinholide, the symmetrical arrangement of the actin subunits bound to lobophorolide is incompatible with the lateral arrangement of actin subunits between protofilaments in models of the F-actin double helix (Holmes et al., 1990), and F-actin nucleation complexes (Reutzel et al., 2004). These commonalities highlight the importance of the ring stacking interaction in formation of the lobophorolide-actin complex and lend support to the functional relevance of the unusual binding stoichiometry observed. However, the covalent connection between the two halves of swinholide likely creates a more stable and more rapidly assembled actin-macrolide complex than that mediated by lobophorolide, which may explain the less complete conversion of monomer to dimer by lobophorolide

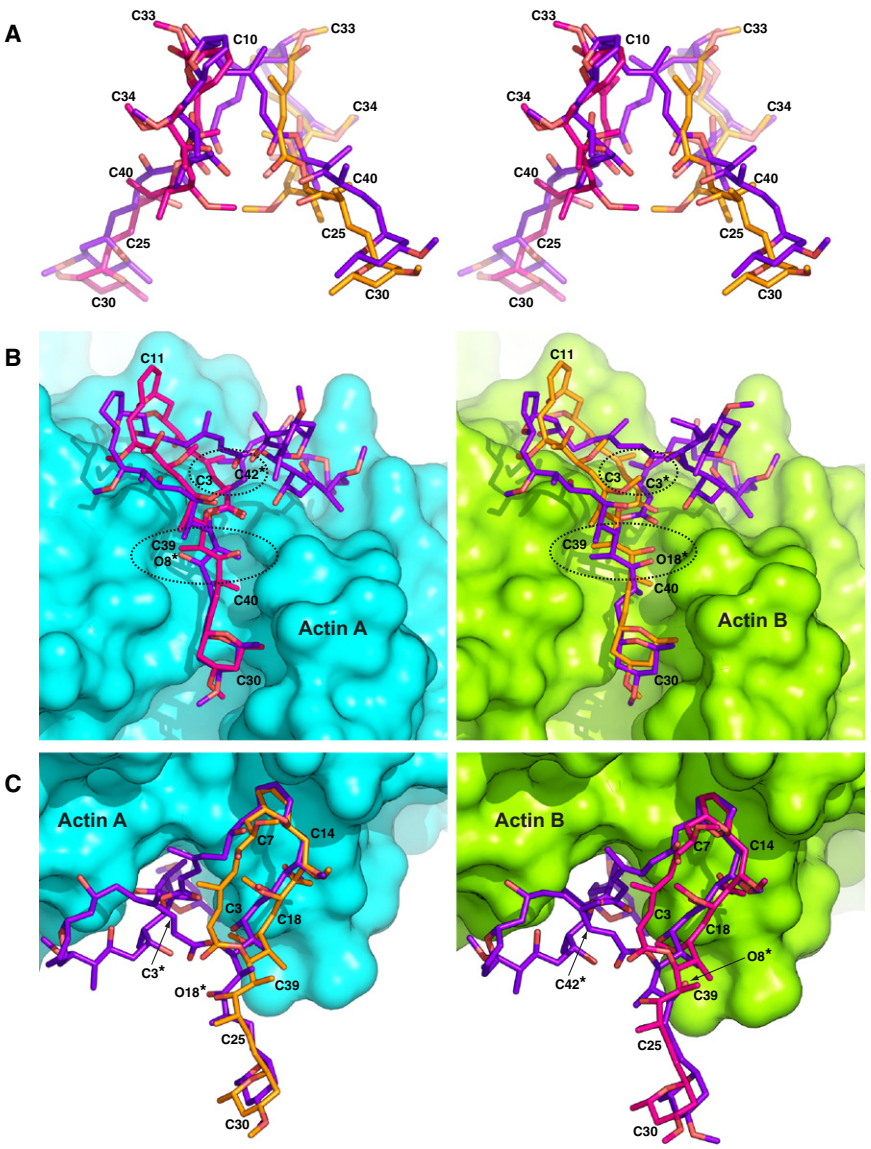

Figure 2. Comparison of Actin Interactions for Lobophorolide and Swinholide A

(A) Stereo view comparison of the two lobophorolide molecules (orange and magenta) and swinholide A (purple, PDB ID: 1QZ5) in their actin-bound configurations.

(B and C) Comparison of the tail and ring-specific interactions of each macrolide with each one of the two actin subunits in the dimer (Actin A and B), respectively. Atom numbers for the swinholide A molecule include asterisks (*). Regions where the conformation of swinholide A is inverted are circled in (B). Alignments for (B) and (C) were performed using the same actin subunit chain for both complexes as shown in the image.

relative to swinholide A in our sedimentation velocity analysis (Figures S2B and S2C). An additional or alternative explanation is that formation of the 2:2 actin-lobophorolide complex is more entropically disfavored than the 2:1 complexation by swinholide A.

Ring-Specific Interactions with Actin

Superposition of the main chains of individual actin subunits from the lobophorolide and swinholide complexes shows that the analogous regions of the lobophorolide ring interact with largely the same surface on both actin subunits as each half of the swinholide ring (Figures 2B and 2C). Interestingly, this alignment also revealed the previously unreported detail that the two halves of swinholide are not identical in their interaction with actin. Hydrophobic interactions between the ring of lobophorolide and the actin subunit bound by its own tail are colored in cyan in Figure 3 and involve residues Gly146, Arg147, Ile330, and Ile345. A hydrogen bond formed between the carbonyl oxygen of Ala144 and O3 in the ring helps stabilize this interaction. Interactions made by the ring with the opposing actin subunit are colored in green in Figure 3 and involve residues Gly23, Asp25, Ile341, Ile345, Ser348, and Leu349. Altogether, these residues compose the binding site of trisoxazole macrolides like kabiramide C in their 1:1 complex with G-actin (Figures S1 and S4) (Klenchin et al., 2003).

The conservation of these interactions across diverse macrolide forms emphasizes the importance of the ring component for actin-macrolide complex formation and underscores the versatility of the corresponding ring binding surface on actin for accommodating different molecular scaffolds. The different roles played by specific regions of the ring of lobophorolide in complex stabilization shows that this element of the macrolide can be divided into several functional subdomains (Figure 3B), and that the structural preorganization provided by the macrocycle permits these individual subdomains to interact across extended binding sites (Driggers et al., 2008). The molecular basis underlying the unique actin subunit-bridging conformation of lobophorolide may be a consequence of other monomeric macrolides not possessing the appropriate arrangement of constituents in their ring to permit actin subunit tethering. Alternatively, due to its smaller size, the lobophorolide ring may lack the conformational freedom required to attain a comparable interaction to other monomeric macrolides with the hydrophobic patch on the surface of the actin subunit to which its tail is bound.

Tail-Specific Interactions and Effects on Actin Polymerization

The actin-binding site of the tail of lobophorolide is highly similar to that of other marine macrolides, especially swinholide A, and

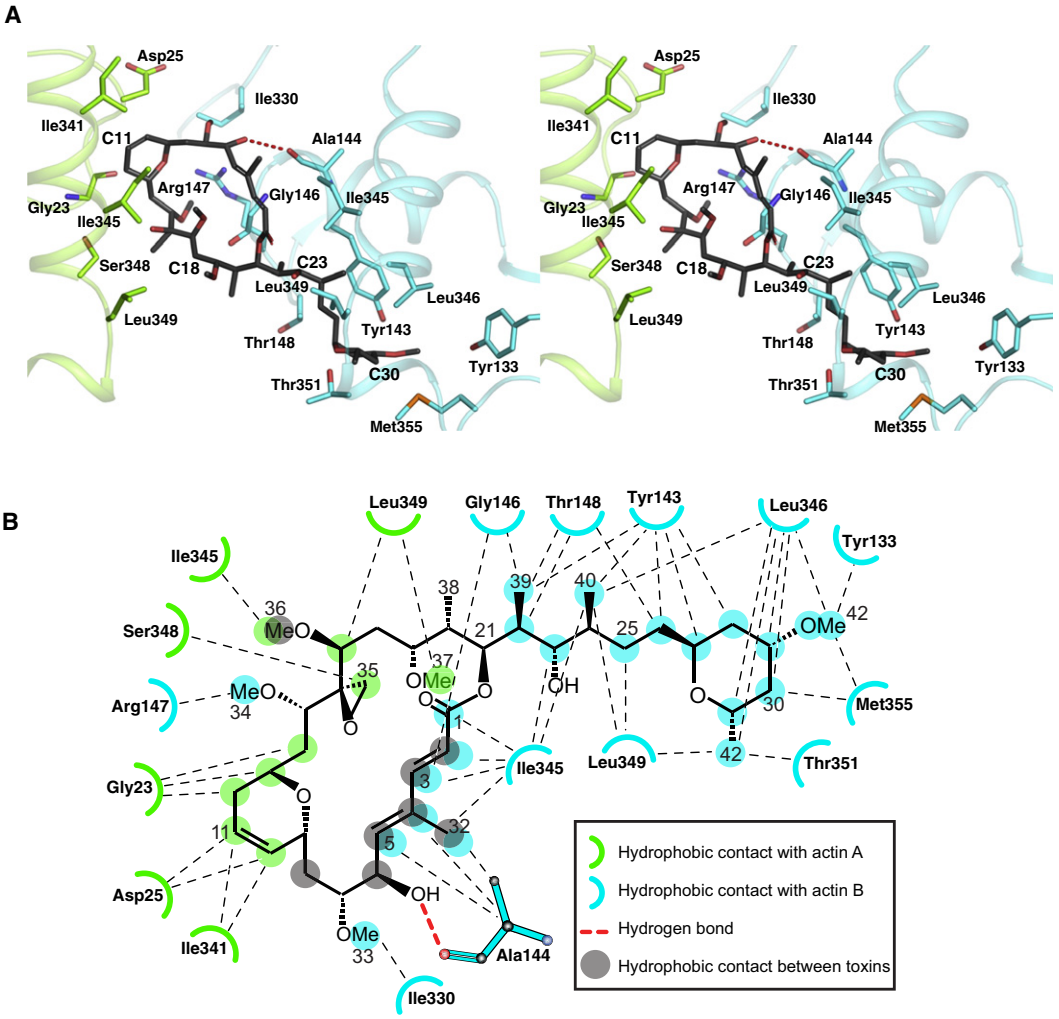

Figure 3. Intermolecular Interactions between the Two Lobophorolide Molecules and Actin

(A) Stereo view of residues from each of the actin subunits (green and cyan) interacting with a single molecule of lobophorolide.

(B) LIGPLOT of the actin-lobophorolide and lobophorolide-lobophorolide contacts.

involves mainly hydrophobic interactions with residues Tyr133, Tyr143, Thr148, Ile345, Leu346, Leu349, Thr351, and Met355 in the barbed end cleft (Figures 2B and 3). These interactions disrupt key protein-protein contacts between the cleft and the DNase I-binding loop of the next actin subunit within the same protofilament (Tirion et al., 1995). In support of this, lobophorolide inhibited polymerization of pyrene-labeled G-actin in kinetic fluorescence assays more potently than mycalolide B, which binds actin with 1:1 stoichiometry (Figure 4A; Figure S1). We also observed that preformed lobophorolide-actin complexes inhibited filament growth, presumably through barbed end capping (Figure 4B; Allingham et al., 2005). Conversely, fluorescence microscopy of AlexaFluor-488-conjugated actin filaments in the presence of macrolides showed that lobophorolide possesses weaker filament severing activity than mycalolide B (Figure 4C). This implies that the main functionality of lobophorolide relies on complexation with G-actin as actin-lobophorolide monomers in which the ring is predisposed to a conformation that presents a self-complementary hydrophobic surface and allows each lobophorolide molecule to share the binding to the other actin subunit, creating an actin filament capping complex. In the absence of a sufficient G-actin pool for dimer formation, as would be the case in our severing assays where most of the actin is filamentous, lobophorolide may only be able to form weak 1:1 interactions with the protofilament subunits, which could account for its less potent actin filament severing activity (Figure 4C). However, the alternative possibility exists that lobophorolide simply lacks potent filament severing activity, regardless of available G-actin, and can indeed form stable 1:1 actin-macrolide complexes. In this regard, the unusual binding stoichiometry we observe may only represent one of a number of possible actin-lobophorolide structural intermediates that could be observed in a crystallization experiment. Nevertheless, based on the marked similarities in macrolide geometry and actin interactions between the lobophorolide and swinholide A complexes, the relevance of the 2:2 binding stoichiometry as

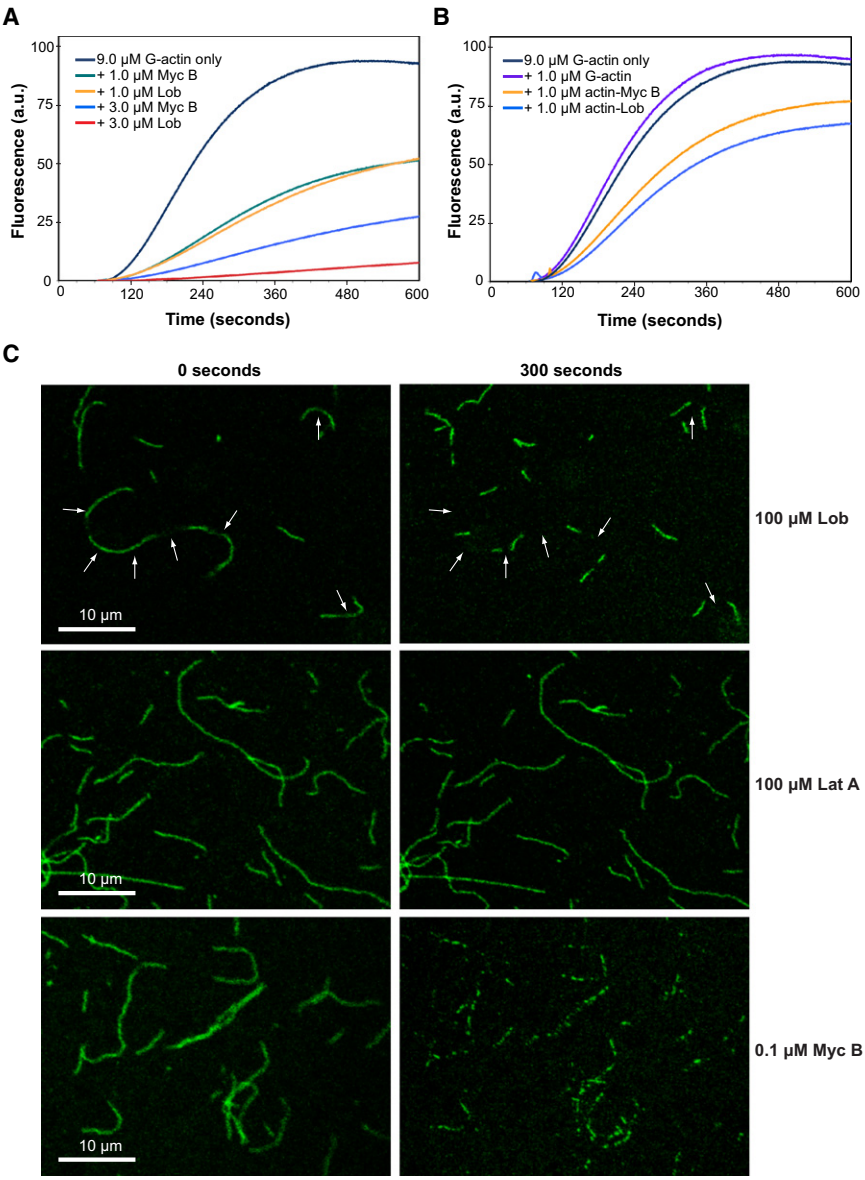

Figure 4. Effects of Lobophorolide on Purified Actin

(A and B) The change in fluorescence signal that occurs during polymerization of 9.0 μM pyrenyl-G-actin in the presence of (A) pure macrolide, or (B) preformed G-actin-macrolide complexes, is plotted as a function of time.

(C) Time-lapse fluorescence microscopy of macrolide-mediated severing of AlexaFluor-488-conjugated actin filaments (indicated by arrows for the lobophorolide treated sample). Macrolide abbreviations are as follows: Lobophorolide (Lob), Latrunculin A (Lat A), and Mycalolide B (Myc B). Latrunculin A was included as a negative control in the severing assays as its activity is limited to actin monomer sequestration (Coue et al., 1987; Spector et al., 1989).

the final, biologically active actin-lobophorolide intermediate is strongly supported.

SIGNIFICANCE

The structure of lobophorolide bound to actin provides a molecular explanation for its dramatic effects on actin polymers in vivo and in vitro (Kubanek et al., 2003). To our knowledge, stabilization of a protein dimer by two separate small molecules with no interaction between the proteins themselves has not previously been observed directly. This discovery highlights the potential for identification of other macrolactone ring-containing small molecules whose functionality involves creation of a dimerization interface for inhibitory or activating protein-protein interactions. It also provides insight into ways to design molecules that tether proteins using different binding surfaces. The similar nature of the ring structure of scytophycins and tolytoxin to lobophorolide suggests that these monomeric macrolides interact with actin with 2:2 stoichiometry as well (Figure S1), and use of their smaller macrocycle scaffolds could have important implications for simplified macrolide mimetic design. Moreover, the remarkable similarities in the chemical and actin-bound structures of lobophorolide and swinholide A support an evolutionary relationship between the two and provides an excellent example where a particular change in a polyketide synthase (PKS) complex can be linked to a biological activity of the small-molecule product (Fischbach et al., 2008). If lobophorolide evolved from a monomeric ancestor that formed a 1:1 complex with actin, then the actin-lobophorolide structure suggests a selective advantage to binding multiple actin molecules. From there, lobophorolide homodimerization to swinholide may have improved the binding affinity to actin.

EXPERIMENTAL PROCEDURES

Detailed Supplemental Experimental Procedures are available online in the Supplemental Information.

Reagents

Actin used in the crystallizations and in vitro assays was purchased from Cytoskeleton Inc. (Denver, CO) and Invitrogen. Lobophorolide was isolated from the brown alga *Lobophora variegata* and harvested at reef locations throughout the Islands of the Bahamas and from the Red Sea near Hurghada, Egypt (Kubanek et al., 2003). Latrunculin A and Mycalolide B were purchased from Sigma (St. Louis, MO) and Alexis Biochemicals, respectively.

Crystallization, Data Collection, and Refinement

Lobophorolide was mixed with 10 mg/ml G-actin from rabbit muscle at a 1:1 molar ratio. Crystals grew from 0.1 M MES (pH 6.0), 6% methyl ether poly (ethylene glycol) 5000, 0.1 M $CaCl_2$, and 1 mM TCEP, and diffraction data were collected at Brookhaven National Labs beamline X6A. Diffraction data were integrated and scaled with the program HKL2000 (Otwinowski and Minor, 1997). The actin-lobophorolide complex structure was solved by molecular replacement from chain A of the actin-swinholide structure (PDB accession code 1XZQ). The structure was refined with Refmac5 and manually optimized using Coot (Emsley and Cowtan, 2004; Murshudov et al., 1997).

Actin Polymerization Inhibition and Filament Severing Assays

The actin polymerization reactions were initiated by the addition of 5 μl of actin polymerization buffer (APB) (100 mM Tris-HCl [pH 7.5], 500 mM KCl, 20 mM MgCl2, and 10 mM ATP) to 45 μl of 9 μM (final concentration) 30% pyrenylactin in G-buffer (Allingham et al., 2005). In one group of treatments the pyrenylactin was incubated with 1 μM of unlabeled actin, actin-mycalolide B, or actin-lobophorolide complexes prepared by incubation of equimolar toxin and unlabeled G-actin. In another group of treatments, the APB contained no toxin, 1 μM toxin, or 3 μM toxin for mycalolide B and lobophorolide. Fluorescence emission at 406 nm was measured using a Lifetime Fluorimeter (ISS, Inc.) with an excitation wavelength of 365 nm.

In vitro severing assays were performed similarly to a protocol previously described in Pavlov et al. (2006). F-actin was prepared by incubating Alexa-Fluor-488-labeled G-actin with unlabelled G-actin in a ratio of 2:5 to a total final concentration of 1.6 μM in F-buffer. F-actin (80 nM) was then applied in F-buffer containing an oxygen scavenging system (4.5 mg/mL D-glucose, 0.2 mg/mL glucose oxidase, 35 μg/mL catalase) to a perfusion chamber where the filaments attached to a glass coverslip through binding to HMM adsorbed to that surface. Actin filaments were visualized in the presence of mycalolides B, lobophorolide or latrunculin A using a Leica TCS SP2 confocal scanning microscope (Mannheim, Germany) with 100× 1.4 numeric aperture oil-immersion optics.

ACCESSION NUMBERS

Coordinates and structure factors for the actin-lobophorolide complex are available in the Protein Data Bank (http://www.rcsb.org/) under ID code 3M6G.

SUPPLEMENTAL INFORMATION

Supplemental Information includes Supplemental Experimental Procedures, four figures, and one table and can be found with this article online at doi:10.1016/j.chembiol.2010.06.010.

ACKNOWLEDGMENTS

We thank M. Fischbach (UCSF) and V. Klenchin (University of Wisconsin, Madison) for helpful discussions, and D. Davis and K. Munro (Queen's University) for technical assistance. J.S.A. was supported by research grants from the Natural Sciences and Engineering Research Council of Canada 356025-08 and the Prostate Cancer Fight Foundation (Motor Cycle Ride for Dad). Use of the National Synchrotron Light Source beamline X6A at Brookhaven National Labs was supported by the National Institute of General Medical Sciences, National Institute of Health under agreement GM-0080 and by the U.S. Department of Energy under contract No.DE-AC02-98CH10886.

Received: March 12, 2010
Revised: May 23, 2010
Accepted: June 8, 2010
Published: August 26, 2010

REFERENCES

Allingham, J.S., Zampella, A., D'Auria, M.V., and Rayment, I. (2005). Structures of microfilament destabilizing toxins bound to actin provide insight into toxin design and activity. Proc. Natl. Acad. Sci. USA *102*, 14527–14532.

Allingham, J.S., Klenchin, V.A., and Rayment, I. (2006). Actin-targeting natural products: structures, properties and mechanisms of action. Cell. Mol. Life Sci. *63*, 2119–2134.

Bubb, M.R., Spector, I., Bershadsky, A.D., and Korn, E.D. (1995). Swinholide A is a microfilament disrupting marine toxin that stabilizes actin dimers and severs actin filaments. J. Biol. Chem. *270*, 3463–3466.

Coue, M., Brenner, S.L., Spector, I., and Korn, E.D. (1987). Inhibition of actin polymerization by latrunculin A. FEBS Lett. *213*, 316–318.

Driggers, E.M., Hale, S.P., Lee, J., and Terrett, N.K. (2008). The exploration of macrocycles for drug discovery–an underexploited structural class. Nat. Rev. Drug Discov. *7*, 608–624.

Emsley, P., and Cowtan, K. (2004). Coot: model-building tools for molecular graphics. Acta Crystallogr. D Biol. Crystallogr. *60*, 2126–2132.

Fischbach, M.A., Walsh, C.T., and Clardy, J. (2008). The evolution of gene collectives: how natural selection drives chemical innovation. Proc. Natl. Acad. Sci. USA *105*, 4601–4608.

Hagelueken, G., Albrecht, S.C., Steinmetz, H., Jansen, R., Heinz, D.W., Kalesse, M., and Schubert, W.D. (2009). The absolute configuration of rhizopodin and its inhibition of actin polymerization by dimerization. Angew. Chem. Int. Ed. Engl. *48*, 595–598.

Hirata, K., Muraoka, S., Suenaga, K., Kuroda, T., Kato, K., Tanaka, H., Yamamoto, M., Takata, M., Yamada, K., and Kigoshi, H. (2006). Structure basis for antitumor effect of aplyronine a. J. Mol. Biol. *356*, 945–954.

Holmes, K.C., Popp, D., Gebhard, W., and Kabsch, W. (1990). Atomic model of the actin filament. Nature *347*, 44–49.

Klenchin, V.A., Allingham, J.S., King, R., Tanaka, J., Marriott, G., and Rayment, I. (2003). Trisoxazole macrolide toxins mimic the binding of actin-capping proteins to actin. Nat. Struct. Biol. *10*, 1058–1063.

Klenchin, V.A., King, R., Tanaka, J., Marriott, G., and Rayment, I. (2005). Structural basis of swinholide A binding to actin. Chem. Biol. *12*, 287–291.

Kobayashi, M., Tanaka, J., Katori, T., and Kitagawa, I. (1990). Marine natural products. XXIII. Three new cytotoxic dimeric macrolides, swinholides B and C and isoswinholide A, congeners of swinholide A, from the Okinawan marine sponge *Theonella swinhoei*. Chem. Pharm. Bull. (Tokyo) *38*, 2960–2966.

Kobayashi, M., Kawazoe, K., Okamoto, T., Sasaki, T., and Kitagawa, I. (1994). Marine natural products. XXXI. Structure-activity correlation of a potent cytotoxic dimeric macrolide swinholide A, from the Okinawan marine sponge Theonella swinhoei, and its isomers. Chem. Pharm. Bull. (Tokyo) *42*, 19–26.

Kubanek, J., Jensen, P.R., Keifer, P.A., Sullards, M.C., Collins, D.O., and Fenical, W. (2003). Seaweed resistance to microbial attack: a targeted chemical defense against marine fungi. Proc. Natl. Acad. Sci. USA *100*, 6916–6921.

Murshudov, G.N., Vagin, A.A., and Dodson, E.J. (1997). Refinement of macromolecular structures by the maximum-likelihood method. Acta Crystallogr. D Biol. Crystallogr. *53*, 240–255.

Otwinowski, Z., and Minor, W. (1997). Processing of X-ray diffraction data collected in oscillation mode. Methods Enzymol. *276*, 307–326.

Pavlov, D., Muhlrad, A., Cooper, J., Wear, M., and Reisler, E. (2006). Severing of F-actin by yeast cofilin is pH-independent. Cell Motil. Cytoskeleton *63*, 533–542.

Perrins, R.D., Cecere, G., Paterson, I., and Marriott, G. (2008). Synthetic mimetics of actin-binding macrolides: rational design of actin-targeted drugs. Chem. Biol. *15*, 287–294.

Pollard, T.D., and Borisy, G.G. (2003). Cellular motility driven by assembly and disassembly of actin filaments. Cell *112*, 453–465.

Reutzel, R., Yoshioka, C., Govindasamy, L., Yarmola, E.G., Agbandje-McKenna, M., Bubb, M.R., and McKenna, R. (2004). Actin crystal dynamics: structural implications for F-actin nucleation, polymerization, and branching mediated by the anti-parallel dimer. J. Struct. Biol. *146*, 291–301.

Spector, I., Shochet, N.R., Blasberger, D., and Kashman, Y. (1989). Latrunculins–novel marine macrolides that disrupt microfilament organization and affect cell growth. I. Comparison with cytochalasin D. Cell Motil. Cytoskeleton *13*, 127–144.

Tirion, M.M., ben-Avraham, D., Lorenz, M., and Holmes, K.C. (1995). Normal modes as refinement parameters for the F-actin model. Biophys. J. *68*, 5–12.

